Electron–phonon coupling in Nb-doped $SrTiO_3$ single crystal

2006 J. Phys.: Condens. Matter 18 2553

(http://iopscience.iop.org/0953-8984/18/8/017)

INSTITUTE OF PHYSICS PUBLISHING JOURNAL OF PHYSICS: CONDENSED MATTER

J. Phys.: Condens. Matter **18** (2006) 2553–2561 doi:10.1088/0953-8984/18/8/017

Electron–phonon coupling in Nb-doped $SrTiO_3$ single crystal

C Z Bi[1,2], J Y Ma[2], J Yan[2], X Fang[2], B R Zhao[2], D Z Yao[1] and X G Qiu[2,3]

[1] Department of Physics, Wuhan University, Wuhan, Hubei 430072, People's Republic of China
[2] National Laboratory for Superconductivity, Institute of Physics, Chinese Academy of Sciences, PO Box 603, Beijing 100080, People's Republic of China

E-mail: xgqiu@aphy.iphy.ac.cn

Received 24 November 2005
Published 10 February 2006
Online at stacks.iop.org/JPhysCM/18/2553

Abstract

Near normal incident infrared reflectivity spectra of (001) $SrTi_{1-x}Nb_xO_3$ single crystal have been measured at different temperatures in the frequency region between 100 and 6000 cm^{-1}. The optical parameters of phonons and plasmons are obtained on the basis of the double-damping extended Drude model. The lowest frequency phonon mode at 175 cm^{-1} softens with decreasing temperature, and the plasmon frequency triples when the temperature decreases from 300 to 10 K. Extra absorption near the highest frequency longitudinal phonon mode shows that the effect of the polarons should be taken into account in addition to the plasmon–phonon coupling. The splitting of the last high reflectivity band, the temperature dependence of the 615 cm^{-1} structure and the appearance of a new weak peak-like defect mode provide evidence for the existence of small polarons.

1. Introduction

The discovery of high T_c superconductivity in copper oxide based perovskite-type materials almost twenty years ago was extraordinarily exciting for both science and technological applications and triggered an extensive search for other superconducting oxides. Strontium titanate with a typical perovskite structure $pm3m$ [1] at room temperature has been known to exhibit a metal–insulator transition [2] upon doping with niobium and become a superconductor [3] with a low electronic concentration at a very low temperature. There is a resurgence of interest in studying the properties of $SrTiO_3$ in conjunction with electron correlation effects in transition metal oxides [4] and due to the close structural relation of the perovskites with high T_c superconductors. As an n-type conductor, $SrTi_{1-x}Nb_xO_3$ is regarded as a bipolaronic superconductivity candidate material [5]. The possibility of polaron

[3] Author to whom any correspondence should be addressed.

formation is obvious due to its huge dielectric polarizability and low carrier density. Some experiments [6–8] have provided evidence for the existence of polarons in $SrTiO_3$. However, there are many unsettled problems as regards the physical properties of n-type $SrTiO_3$, such as how to explain some experimental phenomena like small polarons being indicated by optical properties [9] but effective masses similar to those of large polarons being indicated by heat capacity measurements [10]. Thermoelectric power measurements by Frederikse and co-workers [11] have shown density of states masses to increase from about $6m_e$ to $16m_e$ between 77 and 300 K, which can be explained by a theory of mixed polarons, i.e. large and fairly small polarons [12]. The temperature dependence of plasmons in Nb-doped $SrTiO_3$ has been given by Gervais *et al* [7] and subsequently Eagles and co-workers obtained consistent fitting results using the mixed polaron theory [6]. In the meantime, the role played by polarons in determining the physical properties remains to be clarified, especially with respect the mysterious MIR band. It is of great interest to study the interplay between the phonon, plasmon and polaron in $SrTiO_3$ in particular and strongly correlated oxides in general.

The infrared spectra of $SrTi_{1-x}Nb_xO_3$ reported in the previous papers were incomplete in the low temperature range. The parameters of phonons and plasmons that yielded the best fit to reflectivity data were only provided at room temperature and high temperature in the far infrared region [7]. Moreover, observations and discussions of polarons are few and limited. In this paper we report on the detailed optical properties of $SrTi_{1-x}Nb_xO_3$ at a variety of temperatures, from 300 down to 10 K; the roles played by plasmons and polarons are discussed.

2. Experimental details

One-side-polished single crystal of (100) oriented $SrTiO_3$ doped with 0.9% niobium was provided by Hefei Kejing Co. The infrared reflectivity spectra $R(\omega)$ at different temperatures were measured at near normal incidence of about 8° on a Bomen DA8 Fourier transform infrared spectrometer, in the range from 100 to 6000 cm^{-1}. In the far infrared region, a DTGS detector and a 6 mm Mylar beam splitter were used. In the middle infrared region, a liquid nitrogen cooled mercury cadmium telluride detector and KBr beam splitter were utilized. To obtain the absolute reflectivity, an evaporated gold mirror served as a reference. Spectra were collected with a resolution of 4 cm^{-1}. The samples were mounted in a continuous helium flow cryostat in which the temperature could be varied between 300 and 10 K.

3. Results and discussion

Shown in figure 1 is the temperature dependent reflectivity of the Nb-doped $SrTiO_3$ single crystal at several representative temperatures. The common features of the reflectivity spectra are strong phonon bands peaked in the low frequency range, and a free carrier (plasma) contribution. Four modes can easily be identified at temperatures above 100 K. The three high reflectance bands change with the temperature. Upon lowering the temperature, the whole reflectivity increases; the observed phonon mode at around 175 cm^{-1} softens and finally disappears below 100 K. For the second phonon mode at about 540 cm^{-1}, a blueshift takes place upon cooling and the linewidth decreases, which is considered as an experimental signature of a coupled phonon–plasmon system [13, 7]. At the same time, the high frequency edge of the last band extends to the mid-infrared region in addition to the peak intensity increasing; from 300 to 10 K the reflectivity of the tail decreases above 1850 cm^{-1}. As a result, there is a crossing point in the reflectivity spectrum. Below 100 K a weak absorption band near 780 cm^{-1} appears and becomes more and more obvious with decreasing temperature.

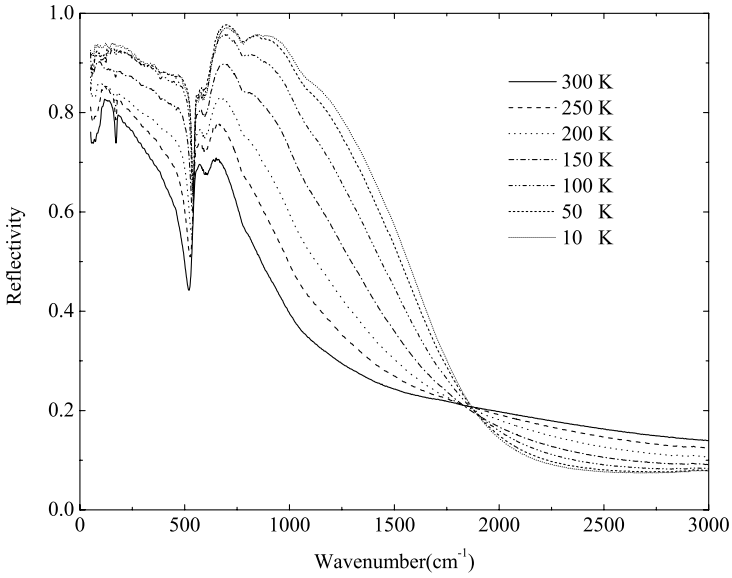

Figure 1. Experimental FIR reflectivity spectra of $SrTi_{1-x}Nb_xO_3$ crystal at various temperatures.

In order to extract the optical parameters of phonons and plasmons, we applied a fitting procedure based on the double-damping extended Drude model (DDD) fit of reflectance spectra with a complex dielectric function $\varepsilon(\omega)$ in the factorized form

$$\varepsilon(\omega) = \varepsilon_1(\omega) + \mathrm{i}\varepsilon_2(\omega) = \varepsilon_\infty \prod_{j=1}^{n} \frac{\omega_{j\mathrm{LO}}^2 - \omega^2 + \mathrm{i}\gamma_{j\mathrm{LO}}\omega}{\omega_{j\mathrm{TO}}^2 - \omega^2 + \mathrm{i}\gamma_{j\mathrm{TO}}\omega} - \frac{\omega_\mathrm{p}^2 + \mathrm{i}\omega(\gamma_\mathrm{p} - \gamma_0)}{\omega(\omega - \mathrm{i}\gamma_0)}, \tag{1}$$

where ε_∞ denotes the high frequency dielectric constant, $\omega_{j\mathrm{TO}}$ and $\omega_{j\mathrm{LO}}$ are the transverse and longitudinal eigenfrequencies of the jth optical phonon mode, and $\gamma_{j\mathrm{TO}}$ and $\gamma_{j\mathrm{LO}}$ their transverse and longitudinal damping constants. ω_p is the plasma frequency, and γ_p is the linewidth of the plasma response at $\omega = \omega_\mathrm{p}$. The parameter γ_0 is the linewidth of the absorption centred at $\omega = 0$. The first term of the right-hand side denotes a pure phonon contribution and the second term a plasmon contribution. With this dielectric function, all the reflectivity spectra in our measurements were fitted with the well-known Fresnel formula:

$$R(\omega) = \left| \frac{\sqrt{\varepsilon(\omega)} - 1}{\sqrt{\varepsilon(\omega)} + 1} \right|^2. \tag{2}$$

On the basis of equations (1) and (2), a fit of $R(\omega)$ to the observed reflectivity spectra can be obtained with a proper choice of the model parameters $\omega_{j\mathrm{TO}}$, $\omega_{j\mathrm{LO}}$, ω_p, $\gamma_{j\mathrm{TO}}$, $\gamma_{j\mathrm{LO}}$, γ_p, γ_0 and ε_∞. Adjustment of the parameters is carried out by trial and error fitting of equation (2) to the experimental spectra. This method yields not only $\varepsilon(\omega)$ but also the model parameters that characterize the infrared active phonons.

Shown in figure 2 are the fitting results at two representative temperatures of 300 and 10 K; the dash–dotted line indicates the experimental FIR reflectivity spectrum and the solid line is the fitting result. Excellent agreement of the fitting to the experimental results is obtained. The fitting parameters are listed in table 1.

Shown in figure 3 is the real part of the optical conductivity versus the wavenumber at different temperatures. The real part of the frequency dependent optical conductivity $\sigma_1(\omega)$ is obtained according to $\sigma_1(\omega) = (\omega/4\pi)\varepsilon_2(\omega)$.

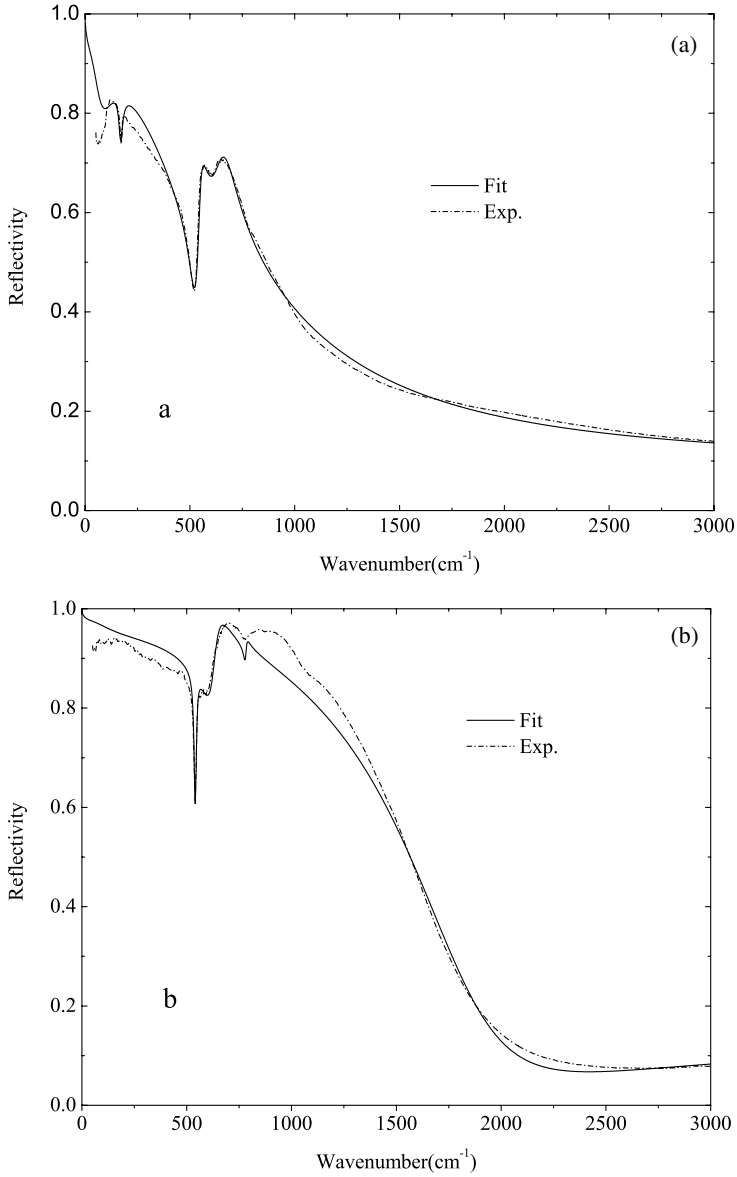

Figure 2. Representative experimental and fitted reflectivity spectra of $SrTi_{1-x}Nb_xO_3$ at (a) 300 K and (b) 10 K. Dash–dotted lines indicate experimental data and solid lines are the fitting results.

When $\omega \rightarrow 0, \sigma_1(\omega)$ from 300 to 10 K is characterized by a Drude component coming from free carriers, rising toward zero photon energy. This agrees well with the fact that σ_{dc} has a metallic behaviour, as shown by the resistance curve in the inset of figure 3. From the band structure calculations for $SrTiO_3$ [14–16], it is well known that the top of the valence band is predominantly dominated by the oxygen 2p states, and the bottom of the unoccupied conduction band has the threefold Ti 3d t_{2g} character, which is a low energy state coming from the original fivefold-orbitally degenerate state and separated from a high energy twofold-orbitally degenerate state (e_g orbitals). The energy gap between the O 2p state and

Table 1. The phonon parameters of the double-damping extended Drude model which yield the best fits to the reflection spectra of $SrTi_{1-x}Nb_xO_3$ single crystal at different temperatures. All units are expressed in cm^{-1}.

Temperature, T (K)		Phonon modes				Plasmon
300	ω_{TO}	137	175	550	640	$\omega_p =$ 545
	γ_{TO}	120	30	24	94	$\gamma_p =$ 1690
	ω_{LO}	165	499	605	1010	$\gamma_0 =$ 40
	γ_{LO}	18	71	190	420	
250	ω_{TO}	135	174	548	634	$\omega_p =$ 615
	γ_{TO}	160	25	20	90	$\gamma_p =$ 1590
	ω_{LO}	167	520	602	1250	$\gamma_0 =$ 40
	γ_{LO}	20	50	175	550	
200	ω_{TO}	135	174	549	634	$\omega_p =$ 855
	γ_{TO}	180	40	17	85	$\gamma_p =$ 1390
	ω_{LO}	164	531	602	1350	$\gamma_0 =$ 40
	γ_{LO}	35	42	175	550	
150	ω_{TO}	135	172	548	636	$\omega_p =$ 1050
	γ_{TO}	190	30	15	80	$\gamma_p =$ 1000
	ω_{LO}	168	536	617	1480	$\gamma_0 =$ 40
	γ_{LO}	28	30	189	550	
100	ω_{TO}	135	548	632	782	$\omega_p =$ 1385
	γ_{TO}	280	14	58	15	$\gamma_p =$ 950
	ω_{LO}	534	628	780	1250	$\gamma_0 =$ 40
	γ_{LO}	30	195	17	200	
50	ω_{TO}	135	548	632	782	$\omega_p =$ 1505
	γ_{TO}	280	15	55	15	$\gamma_p =$ 750
	ω_{LO}	532	625	780	1150	$\gamma_0 =$ 40
	γ_{LO}	39	205	18	200	
10	ω_{TO}	135	547	632	782	$\omega_p =$ 1525
	γ_{TO}	280	13	50	14	$\gamma_p =$ 550
	ω_{LO}	530	615	780	1150	$\gamma_0 =$ 40
	γ_{LO}	37	195	19	230	

the Ti 3d state implies the insulating character of $SrTiO_3$ and the network of corner-sharing TiO_6 octahedra dominates the electronic properties. When Nb is introduced to the system, the transition from Ti^{4+} to Ti^{3+} happens through an electronic compensation mechanism and the creation of oxygen vacancies. From resonant photoemission spectroscopy, Higuchi *et al* have shown that introduced Nb ions will increase the Ti 3d state, and the hybridization between the Ti 3d state and O 2p state is enhanced. An effect of the Nb doping on the energy band is that the Fermi level enters the conduction band [17]. Then the material will show metallic behaviour, which is in agreement with our experimental results. Due to the effect of screening from free carriers, the phonon mode at 175 cm^{-1} exhibits a tendency of weakening and finally disappears at low temperature. Another prominent change is that the plasma frequency ω_p increases sharply by a factor of about 3 upon cooling, which suggests that the effective mass of charge carriers increases due to the relation $\omega_p = 4\pi ne^2/m_e^*\varepsilon_\infty$, assuming that the carrier concentration n is independent of the temperature. Figure 4 shows the linear relationship between the plasma frequency and temperature. At frequency lower than the plasma frequency, total reflection occurs and with decreasing temperature the total reflection region expands to higher energy. The contribution of plasmons to the optical conductivity is depicted in the inset of figure 4. Eagles has calculated this temperature relationship using small polaron [12]

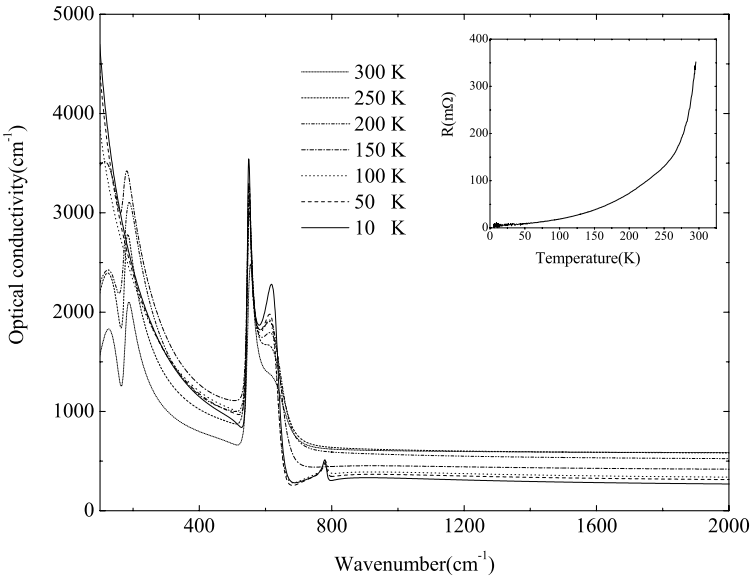

Figure 3. The real part of the temperature dependent optical conductivity of $SrTi_{1-x}Nb_xO_3$ between 10 and 300 K. The conductivity is dominated by the four lattice modes and a free carrier contribution. Shown in the inset is the temperature dependence of the resistance.

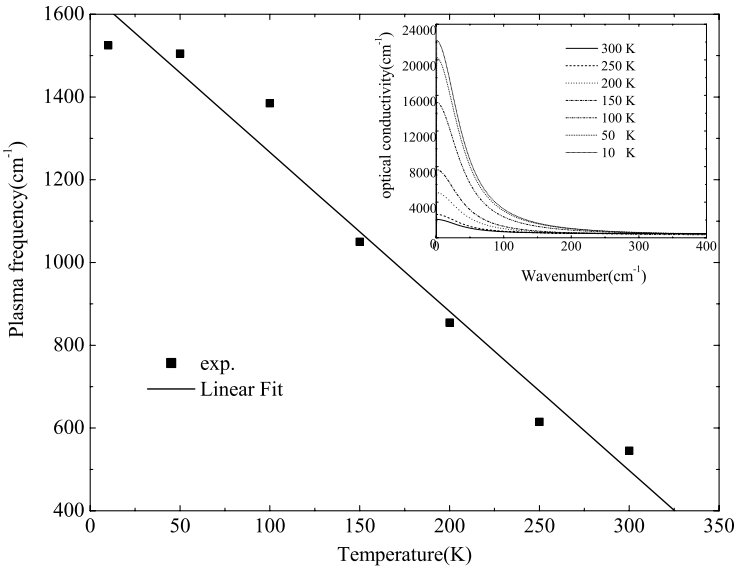

Figure 4. The temperature dependence of the plasma frequency in $SrTi_{1-x}Nb_xO_3$. In the inset, the contributions of plasmons to optical conductivity are shown at various temperatures between 300 and 10 K.

and mixed polaron theory respectively [6]. For the former, there is a discrepancy of about 40% with experimental values at room temperature, and it is contradictory with the transport measurements [11]; for the latter, satisfactory agreement is obtained. Therefore, our results suggest that the mixed polaron theory is more rational.

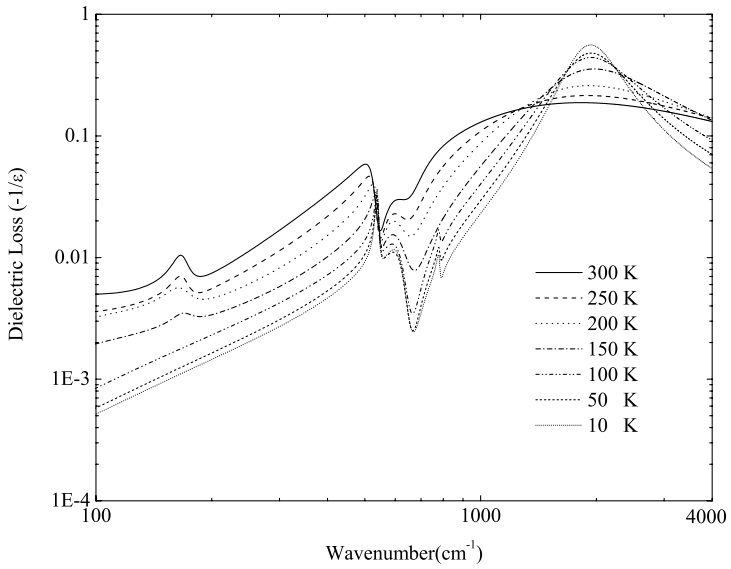

Figure 5. The loss function $\mathrm{Im}[-1/\varepsilon(\omega)]$ at temperatures between 300 and 10 K on a log–log scale.

The peak position in the dielectric loss function, $\mathrm{Im}[-1/\varepsilon(\omega)]$, has been considered as a parameter for plasma excitations of the free carriers. The width of this peak is related to the rate of scattering of the free carriers. Shown in figure 5 is the calculated dielectric loss function. Below 1000 cm^{-1}, the several peaks correspond to frequencies of longitudinal optical phonons ω_{LO}. The peak around 500 cm^{-1} shifts gradually to higher frequency as the temperature decreases, which is probably due to increased plasma frequency [18]. A large mid-infrared (MIR) peak evolves at 2000 cm^{-1} upon lowering the temperature, its intensity enhances with the decreasing temperature. This MIR band has been previously observed in oxygen reduced $SrTiO_3$ and high T_c superconductors, as well as colossal magnetoresistance materials. It has been attributed to the polaron associated with strong electron–phonon coupling. Further work remains to be done to clarify the origin of this MIR band [18–22].

Some of the results mentioned above are in good accordance with previous experiments [7]. But discrepancies exist in the last high reflectance band. Owing to the coupling between the highest frequency phonon mode and the free carrier plasma, the strength and linewidth of the absorption band would change as the temperature decreases. Nevertheless, no splitting has ever been reported. The splitting in our optical conductivity spectra, which is evident even in the room temperature spectrum, can be easily identified. The highest frequency phonon mode evolves into two peaks centred at 550 and 615 cm^{-1} respectively. Furthermore, the high frequency edge of the latter decreases systematically in the mid-infrared region and seems to tail off at low temperature. An additional feature in the reflectivity spectrum near 2000 cm^{-1} was also observed by Barker [23]. He suggested a polaron absorption mechanism. In our measurement, the energy of the polaron may be smaller and close to the phonon energy so that interaction between polarons and phonons could happen. When the polaron absorption peak is imposed on the phonon peak, the splitting of the high frequency reflectivity band can be understood.

On the other hand, the linewidth of the 615 cm^{-1} hump at low temperature narrows and its strength increases. If their origin is the coupling between the plasma frequency and phonon frequency, the high frequency edge of the hump should extend to a larger wavenumber range

at low temperature [24], not shrink on cooling. A favourable candidate for the explanation of the hump is that it is caused by a polaronic characteristic of charge carriers due to the enhanced electron–phonon interaction at low temperature, since a coupling between a plasmon mode and the longitudinal optical phonon modes has been confirmed from the infrared reflectivity spectra. The temperature dependence of the hump is in good agreement with the expected behaviour of polarons [25, 26]. As a result, it may cause the formation of localized bounded states of charge carriers, or small polarons. In contrast, the absorption of large polarons is almost unchanged with temperature change, which is not in agreement with our observation. Another unusual feature is that a weak absorption peak near 780 cm^{-1} develops below 100 K, with its intensity further enhanced slightly at lower temperature. At present, its origin is not clear. To some extent, a peak similar to the defect mode could be related to an oxygen vacancy resulting from Nb doping. That is to say, it could be associated with small polarons, even though it is not very clearly observed above 150 K. The appearance of the peak, which is contradictory with metallic character of $SrTi_{1-x}Nb_xO_3$ because increasing free carrier content will screen those lattice absorption peaks, suggests that polarons are frozen or bounded at low temperature. In Na_xCoO_2, some similar signals have been related to small polarons [27]. In the x-ray absorption spectroscopic (XAS) spectra obtained by Higuchi and co-workers, there are two empty states (denoted as 'a' and 'b') detected below the Fermi level (E_F) in $SrTi_{1-x}Nb_xO_3$. For the state 'a' closer to E_F, its activation energy is estimated from modified photoemission spectroscopic spectra using the Fermi–Dirac distribution. It is of the same order as that of the binding energy, of about 0.1 eV. The energy is very similar to that from our infrared measurement. Moreover, a calculation performed by Sanchez *et al* [28] indicates there to be a slight Nb induced local structure distortion. This kind of distortion as an impurity doping effect has been extensively related to the formation of small polarons in many materials, such as colossal magnetoresistance doped manganites [29–31] and high T_c superconductors [32–34]. Using a quantum chemical model based on the molecular orbital theory, Sanchez *et al* have found that in the crystal, Nb atoms induce the local energy level within the band gap close to the conduction band [35]. Since Nb doping not only makes the Fermi level move into the conduction band as described above, but also changes the band structure near the energy gap, it seems sound that the sub-band is corresponding to the level of small polarons. Therefore, the following conclusions can be reached: that the Nb doping changes the insulator character of STO into metallic behaviour; and at the same time it induces the occurrence of a small polaron energy level below the conduction band. But whether it is originating from local lattice distortion induced by the impurity size effect or the oxygen vacancy is not clear. Anyway, both the positively charged oxygen vacancies and electrons introduced by Nb doping may be energetically favourable for the electrons transfering to the neighbouring Ti^{4+} sites so that they could form Ti^{3+} ions. The strong electron–phonon interaction may cause structural rearrangement that produces a potential minimum: this minimum tends to trap the electron in that orbital and lead to the formation of a 'self-trapped' state called a small polaron. And the small polaron transport is then probably governed by the charge transfer between these Ti^{3+} and Ti^{4+} states. So the above experimental observation and analysis led us to arrive at the following picture for the absorption band close to the mid-infrared range. Small polarons can exist and have an effect on the effective mass of charge carriers in $SrTi_{1-x}Nb_xO_3$ and induce a special absorption peak in the mid-infrared region through electron–phonon interaction.

4. Conclusions

The factorized form of the dielectric function describes well the infrared reflection spectra in Nb-doped strontium titanate at various temperatures. Moreover, a decoupling of the observed

excitations is readily achieved by decomposition of the dielectric function into a sum of pure phonon and plasmon contributions. A splitting takes place in the last high reflectivity band; the 615 cm^{-1} mode changes regularly with temperature and a new mode near 780 cm^{-1} appears at low temperature, which suggests the existence of small polarons and an important role for them in $SrTi_{1-x}Nb_xO_3$.

Acknowledgment

This work was supported by the National Science Foundation (No 10474128).

References

[1] Cox P A 1995 *Transition Metal Oxides* (Oxford: Clarendon)
[2] Calvani P, Capizzi M, Donato F, Lupi S, Maselli P and Peschiaroli D 1993 *Phys. Rev.* B **47** 8917
[3] Schooley J F, Hosler W R and Cohen M L 1964 *Phys. Rev. Lett.* **12** 474
[4] Imada M, Fujimori A and Tokura Y 1998 *Rev. Mod. Phys.* **70** 1039
[5] Mattheiss L F 1972 *Phys. Rev.* B **6** 4740
[6] Eagles D M, Georgiev M and Petrova P C 1996 *Phys. Rev.* B **54** 22
[7] Gervais F, Servoin J L, Baratoff A, Bednorz J G and Binnig G 1993 *Phys. Rev.* B **45** 8187
[8] Ang C, Yu Z, Jing Z, Lunkenheimer P and Loidl A 2000 *Phys. Rev.* B **61** 3922
[9] Reik H G 1967 *Z. Phys.* **203** 346
[10] Ambler E, Colwell J H, Hosler W R and Schooley J F 1966 *Phys. Rev.* **148** 280
[11] Frederikse H P R, Thurber W R and Hosler W R 1964 *Phys. Rev.* **134** A442
Frederikse H P R, Thurber W R and Hosler W R 1966 *J. Phys. Soc. Japan Suppl.* **21** 32
[12] Eagles D M 1985 *Physics of Disordered Materials* ed D Adler (New York: Plenum) p 357
[13] Baumard J F and Gervais F 1977 *Phys. Rev.* B **15** 2316
[14] Van Benthem K, Elsasser C and French R H 2001 *J. Appl. Phys.* **90** 6156
[15] De Groot F M F, Faber J, Michiels J J M, Czyzyk M T, Abbate M and Fuggle J C 1993 *Phys. Rev.* B **48** 2074
[16] Mo S D, Ching W Y, Chisholm M F and Duscher G 1999 *Phys. Rev.* B **60** 2416
[17] Guo X G, Chen X S, Sun Y L, Sun L Z, Zhou X H and Lu W 2003 *Phys. Lett.* A **317** 501
[18] Crandles D A, Nicholas B, Dreher C, Homes C C, McConnell A W, Clayman B P, Gong W H and Greedan J E 1999 *Phys. Rev.* B **59** 12842
[19] Quijada M A, Tanner D B, Chou F C, Johnston D C and Cheong S W 1995 *Phys. Rev.* B **60** 15485
[20] Quijada M A, Tanner D B, Kelley R J, Onellion M, Berger H and Margaritondo G 1999 *Phys. Rev.* B **60** 14917
[21] Lee Y S 2005 *Solid State Commun.* **133** 277
[22] Babonas G J, Bremer J, Dagys R, Hunderi O, Leonyuk L, Pukinskas G, Vetkin A and Wold E 1994 *Physica* C **235** 1129
[23] Barker A S 1976 *Optical Properties and Electronic Structure of Metals and Alloys* ed F Abeles (Amsterdam: North-Holland) p 453
[24] Popovic Z V, De Marzi G, Konstantinovic M J, Cantarero A, Dohcevic-Mitrovic Z, Isobe M and Ueda Y 2003 *Phys. Rev.* B **68** 224302
[25] Emin D 1975 *Adv. Phys.* **24** 305
[26] Yoon S, Liu H L, Schollerer G, Cooper S L, Han P D, Payne D A, Cheong S W and Fisk Z 1998 *Phys. Rev.* B **58** 2795
[27] Wang N L, Wu D, Li G, Chen X H, Wang C H and Luo X G 2004 *Phys. Rev. Lett.* **93** 147403
[28] Sanchez P and Stashans A 2002 *Phys. Status Solidi* b **230** 397
[29] Mills A J, Littlewood P B and Shraiman B I 1995 *Phys. Rev. Lett.* **74** 5144
[30] Mills A J, Mueller R and Shraiman B I 1996 *Phys. Rev.* B **54** 5405
[31] Roder H, Zang J and Bishop A R 1996 *Phys. Rev. Lett.* **76** 1356
[32] Calvani P, Capizzi M, Lupi S, Maselli P and Paolone A 1996 *Phys. Rev.* B **53** 2756
[33] Lupi S, Calvani P, Capizzi M, Maselli P, Sadowski W and Walker E 1992 *Phys. Rev.* B **45** 12470
[34] Thomas G A, Rapkine K H, Cooper S L, Cheong S W, Cooper A S, Schneemeyer L F and Waszczak J V 1992 *Phys. Rev.* B **45** 2474
[35] Sanchez P and Stashans A 2003 *Mater. Lett.* **57** 1844